

Local structure of the B-site in BNT-xBT investigated by $^{47,49}\text{Ti}$ NMR: Effect of barium content

Cite as: J. Appl. Phys. **121**, 114104 (2017); <https://doi.org/10.1063/1.4978017>

Submitted: 06 December 2016 . Accepted: 22 February 2017 . Published Online: 20 March 2017

Pedro B. Groszewicz, Hergen Breitzke, Wook Jo, et al.



View Online



Export Citation



CrossMark

ARTICLES YOU MAY BE INTERESTED IN

[On the phase identity and its thermal evolution of lead free \$\(\text{Bi}_{1/2}\text{Na}_{1/2}\)\text{TiO}_3\$ -6 mol% \$\text{BaTiO}_3\$](#)

Journal of Applied Physics **110**, 074106 (2011); <https://doi.org/10.1063/1.3645054>

[Ca doping in \$\text{BaTiO}_3\$ crystal: Effect on the Raman spectra and vibrational modes](#)

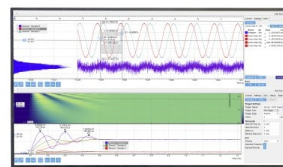
Journal of Applied Physics **121**, 114102 (2017); <https://doi.org/10.1063/1.4978507>

[Observation of ferroelectric phase and large spontaneous electric polarization in organic salt of diisopropylammonium iodide](#)

Journal of Applied Physics **121**, 114101 (2017); <https://doi.org/10.1063/1.4978515>

Challenge us.

What are your needs for periodic signal detection?



Zurich
Instruments

Local structure of the B-site in BNT-xBT investigated by $^{47,49}\text{Ti}$ NMR: Effect of barium content

Pedro B. Groszewicz,¹ Hergen Breitzke,¹ Wook Jo,² Jürgen Rödel,^{3,a)} and Gerd Buntkowsky^{1,a)}

¹Institute of Physical Chemistry, Technische Universität Darmstadt, 64287 Darmstadt, Germany

²School of Materials Science and Engineering, Ulsan National Institute of Science and Technology, 689-798 Ulsan, South Korea

³Institute of Materials Science, Technische Universität Darmstadt, 64287 Darmstadt, Germany

(Received 6 December 2016; accepted 22 February 2017; published online 20 March 2017)

Towards a deeper understanding of the local structure of the B-site in $(100-x)(\text{Bi}_{1/2}\text{Na}_{1/2})\text{TiO}_3-x\text{BaTiO}_3$ (BNT-xBT) with $0 \leq x \leq 15$, solid-state nuclear magnetic resonance (NMR) spectra of the titanium isotopes ^{47}Ti and ^{49}Ti were investigated. The $^{47,49}\text{Ti}$ NMR spectra of BNT-xBT indicate a disordered local structure for the B-site of these perovskites. The line-shape of the titanium NMR spectra of BNT-xBT samples is found to be independent on the barium content. This fact implies that the local structure of the B-site remains invariant with respect to the structural changes that result from the chemical modification with barium. The analysis of $^{47,49}\text{Ti}$ NMR spectra supports the hypothesis that the main structural changes across the morphotropic phase boundary in these solid-solutions are constrained to the A-site and are related to the tilting of rigid oxygen octahedra. Published by AIP Publishing. [<http://dx.doi.org/10.1063/1.4978017>]

INTRODUCTION

Titanium is an element ubiquitous in materials of technological and scientific interest. Titanium oxide moieties (TiO_6) are an important building block of many ceramic materials with favorable mechanical and electrical properties, as, for example, the piezoelectric ceramic $\text{Pb}(\text{Zr}_x, \text{Ti}_{1-x})\text{O}_3$ (PZT)¹ and one of its lead-free counterparts $(100-x)(\text{Bi}_{1/2}\text{Na}_{1/2})\text{TiO}_3-x\text{BaTiO}_3$ (BNT-xBT).^{2,3}

The macroscopic properties of these materials are closely related to their structure at the atomic level. For example, the ferroelectricity of BaTiO_3 is a consequence of the displacement of Ti^{4+} cations out of the center of the oxygen octahedra present in the perovskite structure.⁴ The direction of this displacement is a function of temperature and determines the structure of the polymorphs observed for BaTiO_3 upon cooling from the Curie temperature (T_c).⁴⁻⁶

Solid-state nuclear magnetic resonance (NMR) is a spectroscopic technique highly sensitive to this kind of symmetry breaking. It was previously employed to study the polymorphs of BaTiO_3 , and it was able to characterize the symmetry changes that occur to the local structure of the titanium site upon cooling from T_c .⁷ This feature of NMR was also employed to reveal the presence of polar nanoregions (PNRs) in both lead-based⁸ and lead-free⁹ relaxor ferroelectrics. More recently, solid solutions of BNT-xBT were investigated with ^{23}Na NMR and density functional theory (DFT) calculations.¹⁰ This study showed that the local structure of the A-site is heavily influenced by tilting of oxygen octahedra, which are suppressed by the addition of barium. Furthermore, the relaxor properties of BNT-xBT, which show a peculiar composition dependence between

$0 < x\text{BT} < 15$, were found to correlate with a pronounced degree of disorder in octahedra tilting.¹⁰

Despite the broad technical and scientific interest in titanium-based oxides, $^{47,49}\text{Ti}$ solid-state NMR is not yet a widespread technique for their structural characterization. Padro *et al.* made a very comprehensive $^{47,49}\text{Ti}$ NMR investigation of titanium in oxides,¹¹ among which $(\text{Bi}, \text{Na})\text{TiO}_3$ and BaTiO_3 are also mentioned. Both titanium isotopes (^{47}Ti and ^{49}Ti) are quadrupolar nuclei with relatively low gyromagnetic ratio. Their resonance frequencies differ only by 266 ppm.¹² This proximity is one of the challenges of titanium NMR, as signals from both isotopes might overlap, depending on the magnitude of the external magnetic field and electric field gradient (EFG) on the titanium site. A second challenge is the low natural abundance of the NMR active isotopes of titanium, which results in low sensitivity for signal detection. Typical measurement times of several days may be required for acquiring a $^{47,49}\text{Ti}$ solid-state NMR spectrum, despite the relatively fast relaxation rates of these quadrupolar nuclei.

Regardless of these challenges, titanium NMR is a powerful analytical method sensitive to the local structure. The $^{47,49}\text{Ti}$ chemical shift ranges from +1278 ppm for TiI_4 ¹² to -1389 ppm for $\text{Ti}(\text{CO})_6$ ¹³ and serves as a fingerprint of the nature of neighboring atoms. More specifically, ABO_3 materials with TiO_6 moieties resonate in the spectral range between -850 ppm (CaTiO_3) and -690 ppm (PbTiO_3).¹⁴

The quadrupolar coupling renders titanium NMR sensitive to the symmetry around this nucleus. For non-symmetric local environments, the line-shape of the $^{47,49}\text{Ti}$ solid-state NMR spectrum is determined by the strong first and second order quadrupolar interactions, which result from the electric field gradient at the nucleus' site. In a site of cubic local symmetry, the EFG and the quadrupolar interaction vanish, resulting in characteristic changes in the NMR spectrum,

^{a)}Electronic addresses: roedel@ceramics.tu-darmstadt.de and gerd.buntkowsky@chemie.tu-darmstadt.de

analogous to those employed for the quantification of a cubic phase in BNT-xBT by means of ^{23}Na NMR.⁹

The local symmetry of perovskites at room temperature depends on the size-ratio between the A-site and B-site cations, expressed as the tolerance factor.¹⁵ BaTiO_3 is representative of perovskites with a tolerance factor larger than unity (i.e., a too large an A-site cation is present) and its structure is stabilized by ionic displacements of Ti^{4+} relative to the oxygen lattice. In the high-temperature phase, this compound exhibits the prototypical cubic $Pm\bar{3}m$ structure. With decreasing temperature, phase transitions into tetragonal $P4mm$,⁴ orthorhombic $Amm2$,⁶ and rhombohedral $R3m$ ⁵ structures occur. The displacement of Ti^{4+} from the center of the oxygen octahedra causes an EFG > 0 at this site, which is reflected in the width and shape of the $^{47,49}\text{Ti}$ NMR signal. More specifically, $^{47,49}\text{Ti}$ NMR lines reported for the rhombohedral polymorph of BT are twice as broad as for the tetragonal one.⁷

For perovskites where the A-site is occupied by a too small a cation (i.e., tolerance factor lower than unity), tilting of TiO_6 octahedra occurs as another mechanism of symmetry lowering.^{16,17} Due to the connectivity between the oxygen octahedra, their rotation resembles a cogwheel mechanism. The tilting may occur along one or more crystallographic axes and may be either in-phase or anti-phase. These characteristics allow octahedra tilting to be categorized in tilt systems, which are conveniently described by Glazer's notation.¹⁶ While tilting impacts the macroscopic symmetry of perovskites, on a local scale, it mainly influences the A-site. The titanium nuclei poised in the B-site in the middle of oxygen octahedra remain insensitive to their tilting as a rigid unit. This mechanism is found, for instance, in $(\text{Bi}_{1/2}, \text{Na}_{1/2})\text{TiO}_3$ (BNT).¹⁸

The chemical modification of BNT with barium is a key aspect to achieve enhanced dielectric and piezoelectric properties in BNT-xBT solid-solutions.^{3,19} It also influences the average structure of the material and causes a series of composition-induced phase transitions.^{20,21} More specifically, BNT-xBT may present either a rhombohedral ($x < 5$) or tetragonal structure ($x > 11$), depending on the barium content.²¹ These regions of the phase diagram are separated by an intermediate region ($5 \leq x \leq 11$) with predominantly relaxor features. If poled, the so-called morphotropic phase boundary (MPB), which encompasses the compositions with largest piezoelectric coefficients among these lead-free ceramics, is located at about $x = 6$.²⁰

MPB compositions have been the focus of intense research, as the structural features responsible for the enhanced piezoelectricity of BNT-xBT are still unclear. If the MPB of BNT-xBT is analogous to the one of PZT, rhombohedral and tetragonal displacements of the B-site cation should coexist. In this case, the different symmetries observed for the average structure as a function of barium content should influence the local structure of Ti^{4+} and, hence, impact the $^{47,49}\text{Ti}$ NMR lines in analogy to the polymorphs of BaTiO_3 . However, if the chemical modification with barium mainly influences the structure of BNT by changing the tilting of octahedra, the local structure around the titanium nuclei is expected to remain invariant throughout the different regions of the phase diagram of BNT-xBT.

Therefore, the focus of the present study is to investigate how the addition of barium to BNT impacts the local structure of the titanium site. Towards this goal, we analyze solid-state $^{47,49}\text{Ti}$ NMR spectra of BNT-xBT with $x = 0, 6, 15$. These compositions are representative of the rhombohedral, the morphotropic phase boundary (MPB), and the tetragonal regions from the phase diagram of this solid-solution. The comparison between their $^{47,49}\text{Ti}$ NMR spectra casts new light on the structural changes across the MPB, as it is demonstrated that the addition of barium cations does not significantly change the local structure of the B-site in these perovskites.

EXPERIMENTAL

$^{47,49}\text{Ti}$ NMR spectra were recorded with a Varian CMX 600 Infinity+ spectrometer at a frequency of 33.810800 MHz. A Varian 5 mm magic angle spinning (MAS) triple resonance probe was employed for both static and magic angle spinning (MAS) measurements. In order to measure at the low resonance frequency required for the observation of titanium NMR-active isotopes, this probe was modified with two additional capacitors of 50 pF on the Y channel, which was connected to the X channel via a shunt. While for MAS experiments the sample was packed into a 5 mm ZrO_2 rotor, static experiments made use of a thin-walled 5 mm glass NMR tube to achieve a larger filling factor of the coil. The $^{47,49}\text{Ti}$ NMR chemical shift scale is referenced with the ^{49}Ti resonance of neat $\text{TiCl}_4(\text{l})$ at 0 ppm.¹² Spectra of TiO_2 and BaTiO_3 were simulated with the DmFit program.²²

In a first attempt, the original DEPTH (90-180-180) pulse sequence²³ was employed for the $^{47,49}\text{Ti}$ NMR measurements, to remove spectral artifacts caused mainly by acoustic ringing of the probe. While it already gave a good suppression of the acoustic ringing of the probe, this artifact still hindered the acquisition of faster decaying signals (i.e., whenever the quadrupolar coupling broadened the spectra significantly). Therefore, the modified ECHODEPTH sequence 90-180- τ -180- τ , which uses the same phase cycling as the original DEPTH²³ sequence, was developed. The additional delay τ between the two π pulses of the DEPTH sequence generates an echo (see the [supplementary material](#) for details), which further removes dead-time artifacts.²⁴ It is found that the ECHODEPTH sequence suppresses the effects of the acoustic ringing much better than the simple DEPTH sequence, thus allowing the detection of fast-decaying signals. A pulse length of 3 μs was employed for the π pulses resulting in an excitation profile of ca. 300 kHz. For a typical experiment, 460 000 scans were recorded with a recycle delay of 0.5 s. The echo delay for static experiments was equal to 100 μs , taking into account the pulse lengths. For MAS experiments, the echo delay was synchronized to one rotor period. Since there are no resolved side-bands or satellite transitions visible in the spectra of the BNT-xBT materials, only the region of the central transition is shown.

RESULTS

The Results section is structured as follows: first, the $^{47,49}\text{Ti}$ NMR spectra of known materials are analyzed in order to validate the ECHODEPTH sequence and to test the

response of the NMR probe. Next, the spectra of BaTiO₃ and a BNT-xBT sample are compared, followed by the investigation of titanium NMR spectra of BNT-xBT as a function of the barium content.

Reference substances

Our experimental approach, in particular, the modified DEPTH sequence, is validated by recording the spectra of known samples with increasingly broader lines: first, the “easy-to-record” SrTiO₃, then TiO₂ under MAS and at last BaTiO₃. For the latter, resonances from both titanium isotopes overlap under static conditions. Figure 1 displays the ^{47,49}Ti NMR spectra of SrTiO₃ (a) and TiO₂ anatase (b), both measured under MAS frequencies of 10 kHz. In addition, the static spectrum of BaTiO₃ is displayed in Figure 1(c).

The spectrum of SrTiO₃ (Figure 1(a)) presents two sharp and intense peaks at −842 ppm and −1108 ppm that correspond to the resonances of ⁴⁹Ti and ⁴⁷Ti isotopes, respectively. Both titanium NMR signals of SrTiO₃ are very narrow, as a consequence of its well defined cubic structure and the resulting absence of features from the quadrupolar interaction in the spectrum.²⁵

Resonances from both isotopes are also present in the MAS spectrum of TiO₂ (Figure 1(b)), which exhibit the typical shape for the quadrupolar interaction with a well-defined local structure. An important feature of the central transition of a 2nd order quadrupolar perturbed spectrum is its characteristic shape with distinct maxima and abrupt singularities. These features are related to the anisotropy of the quadrupolar interaction, which cannot be fully averaged for powder samples under MAS at the magic angle of 54.7°. Despite the high level of noise, singularities can be recognized on the edges of the central transition for both isotopes as a sudden, almost vertical, intensity change.

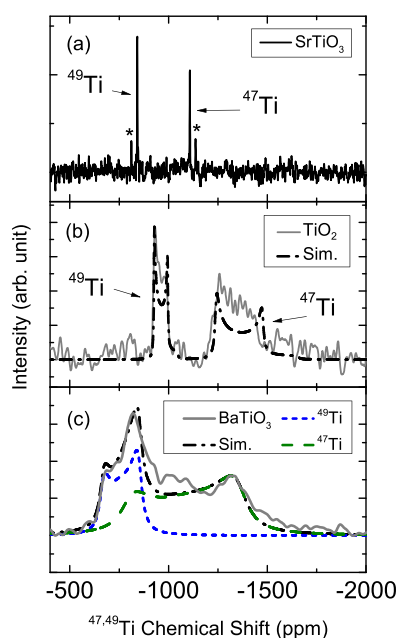


FIG. 1. ^{47,49}Ti MAS NMR spectra of SrTiO₃ (a) and TiO₂ (b), with MAS spinning frequency of 10 kHz, followed by the static spectrum of BaTiO₃ (c). Simulations of spectra are denoted by dashed/dotted lines.

The NMR parameters of TiO₂ can be extracted from the spectrum by fitting the position of these singularities with simulated ^{47,49}Ti NMR spectra (Figure 1(b)—dashed-dotted line). During this procedure, special attention was paid to the line of the ⁴⁹Ti isotope. Its simulation revealed an isotropic chemical shift of −906 ppm and a quadrupolar coupling constant (C_Q) of about 5 MHz. These values agree with the reported NMR parameters of TiO₂ anatase.^{25,26} Moreover, the line simulated for the ⁴⁷Ti isotope with these parameters yields a width similar to the experimental one.

The experimental approach was also validated for static conditions, by recording a spectrum of BaTiO₃ without MAS spinning (Figure 1(c)). The static ^{47,49}Ti NMR spectrum of BaTiO₃ presents a peak around −800 ppm and two singularities at −600 ppm and −1400 ppm. The presence of these abrupt singularities is the consequence of the well-defined local environment of titanium nuclei in the tetragonal phase of BaTiO₃. These features also enable the simulation of the individual spectrum of each isotope, displayed in Figure 1(c) as dotted/dashed lines. Special attention was paid in simulating the complete width of the spectrum. It was found that the lines of ⁴⁹Ti and ⁴⁷Ti overlap slightly at this magnetic field. Despite that, the high-field singularity can be attributed to the ⁴⁷Ti resonance, whereas the low-field singularity corresponds to the ⁴⁹Ti resonance. Besides reproducing both singularities, the simulation also mimics the peak close to −800 ppm, which arises from signals where both isotopes overlap. By a visual fit of the spectra with simulations, an isotropic chemical shift of −725 ppm and a C_Q of about 4.0 MHz result for the ⁴⁹Ti isotope. These values are close to those reported in the literature ($C_Q = 3.76$ MHz) for this isotope in BaTiO₃ at room temperature.^{7,27} The analysis of reference materials supports the validity of the ECHODEPTH sequence for recording NMR spectra of titanium under static and MAS conditions.

BNT-xBT materials

Next, the static ^{47,49}Ti NMR spectra of BaTiO₃ and BNT-15BT are compared (Figure 2). The signal of the central transition appears in the same region of chemical shift in both spectra. This is an evidence of the similar chemical environment around the titanium nuclei in both materials. Besides that, the spectrum of BNT-15BT presents some

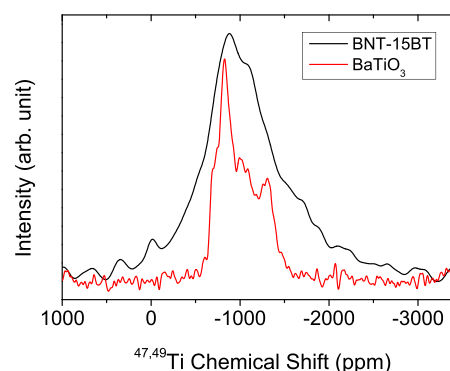


FIG. 2. Static ^{47,49}Ti NMR spectra (central region) of BaTiO₃ (red) and BNT-15BT (black).

remarkable features that contrast to the spectrum of BaTiO_3 . First, the signal for BNT-15BT does not exhibit the steep singularities as those observed for BaTiO_3 and TiO_2 . Second, the high-field side of the signal is less steep than the low-field side. Both observations are a clear indication of a distribution of solid-state NMR parameters (especially C_Q and η), as reported for solid-solutions of $(\text{Ba}_{1-x}\text{Sr}_x)\text{TiO}_3$.²⁸ In addition to that, the distinct maxima expected for a quadrupolar nucleus in a single, well-defined EFG are not observed. Instead, one broad maximum at -880 ppm is present. Altogether, these features indicate a disordered local structure for the titanium site in BNT-15BT.

In order to investigate the effect of barium on the local structure of BNT-xBT ceramics, titanium NMR spectra were recorded for samples with different barium content, namely, for pure BNT, BNT-6BT, and BNT-15BT. Their static spectra are displayed in Figure 3(a). The same features described for the spectrum of BNT-15BT in Figure 2 can be observed in the spectra of pure BNT and BNT-6BT. From Figure 3, it is evident that the line-shape of the spectra and thus the local quadrupolar interaction and the local chemical environment of the titanium nuclei are practically independent of the amount of barium in the sample. The structural meaning of this independence is discussed below.

To gain further insight into the materials, the MAS spectra of the sample with the lowest (BNT-0BT) and highest (BNT-15BT) barium content were recorded (Figure 3(b)). Sample spinning under MAS induces a narrowing of the lines, due to partial averaging of the anisotropic NMR interactions between the nuclei and the local structure. The maximum exhibited by the static spectra is present as two peaks in the MAS spectra (Figure 3(b)), which occur at -920 ppm and -1170 ppm, respectively. The difference of approximately 250 ppm is close to the separation expected between the lines of both isotopes. Hence, these maxima can be attributed to the lines of both NMR-active titanium isotopes,

instead of a feature of the quadrupolar coupling 2nd order for a single isotope.

^{47,49}Ti NMR lines present approximately the same width for all three compositions. Under static conditions, the fwhm is approximately 770 ppm, whereas the spectra recorded under MAS exhibit a fwhm of 520 ppm. In addition, a broad hump between 0 and -2500 ppm (84 kHz broad) is present in the MAS spectra. The broader part of the MAS spectra is similar to the lower portion of the static spectra of BNT-xBT.

The comparison between static and MAS spectra indicates a distribution of both the quadrupolar coupling constant C_Q and the asymmetry parameter η and thus also the components of the EFG tensor. MAS will only effectively narrow the central transition lines in powder samples if the spinning frequency surpasses the width of the central transition (in frequency units) under static conditions.²⁹ The spectrum of a material for which a distribution of C_Q is present is the weighed sum of the lines for each value of C_Q in the distribution. If the spinning frequency is smaller than the width of the broadest line under the distribution, sites with different C_Q will behave differently under MAS. While the sites with C_Q smaller than the threshold value will be effectively narrowed, the sites with larger C_Q will remain with the same width as in the static spectrum, and result in a broad hump, as the one observed in Figure 3(b).

DISCUSSION

The results of our previous NMR investigation of BNT-xBT¹⁰ assume that oxygen octahedra tilt as rigid units, with tilting governed by the barium content. Based on this premise, the ^{47,49}Ti NMR spectra should remain unchanged for compositions with different barium content in the range from 0% to 15%. The ^{47,49}Ti NMR spectra of BNT-xBT samples, measured under static conditions (Figure 3(a)), do not present any significant changes as a function of barium content, indeed. Lines for BNT-0BT, BNT-6BT, and BNT-15BT all appeared in the same frequency range, revealing the same maximum position and a very similar line width.

The spectral features of the central transition of the titanium NMR lines are mainly determined by the chemical shift and the 2nd order quadrupolar interactions, which are expressed in terms of the isotropic chemical shift (δ_{ISO}) and the quadrupolar coupling constant (C_Q), respectively. These NMR parameters are associated with the local structure of the titanium site, with correlations to specific structural features being reported for ABO_3 oxides. The values of the isotropic chemical shift are related to mean Ti-O distances, whereas the shear strain in the TiO_6 octahedra (based on bond angle of O-Ti-O bonds) exhibits a strong correlation with the magnitude of the quadrupolar coupling.¹⁴ The shear strain is related to both titanium displacements and oxygen octahedra distortions, characterizing the C_Q as a spectral parameter sensitive to the local symmetry around this cation.

BNT-xBT samples with different barium content exhibit different symmetries for the average structure.^{3,20,21,30} Rhombohedral and tetragonal regions of its phase diagram are separated by a morphotropic phase boundary (MPB) around a barium content of 6%. Hence, one could expect

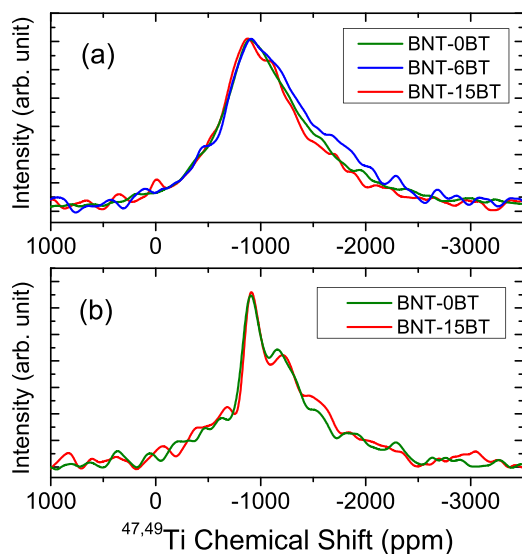


FIG. 3. ^{47,49}Ti NMR spectra of BNT-xBT. (a) Static and (b) under MAS (central region, spinning frequency of 10 kHz, corresponding to ca. 265 ppm).

some kind of change at the local structure of the B-site across the MPB, which would impact the structure-relevant NMR parameters, and in their turn, the spectra. The sensitivity of $^{47,49}\text{Ti}$ NMR to such changes is evidenced by an analogy to the rhombohedral and tetragonal polymorphs of BaTiO_3 , as the latter exhibits lines with half the width of the former, due to its lower C_Q value.⁷ With respect to this, the lack of changes in the titanium NMR spectra of BNT-xBT as a function of composition implies that the differences in local structures around the titanium ions are too small to be revealed by $^{47,49}\text{Ti}$ NMR. This is a highly relevant result, as it confirms the interpretation from our previous ^{23}Na NMR investigation of BNT-xBT¹⁰ that TiO_6 units behave as rigid octahedra when the addition of barium suppresses their tilting.

Furthermore, the lack of clear singularities and the line-shape of the $^{47,49}\text{Ti}$ static spectra of BNT-xBT indicate a distribution of NMR parameters, in particular, of the C_Q values. This emphasizes that the local structure around titanium cations in BNT-xBT is marked by a significant structural disorder. Similar results were reported in a ^{137}Ba NMR study of the A-site disordered $(\text{Ba}_{1-x}, \text{Sr}_x)\text{TiO}_3$ perovskite.²⁸

Both conclusions are in agreement with the x-ray absorption fine-structure (XAFS) measurements of the local structure of $(\text{K}_x\text{Na}_{1-x})_{0.5}\text{Bi}_{0.5}\text{TiO}_3$ (BNT-BKT).³¹ In that work, the Ti edge XANES signal was investigated as a function of K^+ content. Its authors observed only very slight changes in the magnitude of Ti displacements when varying the potassium content along compositional phase transitions. Since x-ray absorption near edge structure (XANES) data could not be fitted with either [100] or [111] displacements, a radial distribution of Ti displacements was proposed. Such a disordered scenario is well reflected by the shape of titanium NMR lines analyzed in the scope of the present work. A more recent EXAFS investigation of BNT also revealed that the local environment around the titanium site does not change as a function of temperature and poling state.³²

In addition, the $^{47,49}\text{Ti}$ NMR spectra presented here support the conclusions from a recent investigation of the local structure of the A-site of BNT-xBT using ^{23}Na NMR.¹⁰ DFT calculations revealed that the EFG on the sodium site of these perovskites is mainly influenced by tilting of octahedra. In this previous work, it was also demonstrated that the addition of barium caused a marked decrease in the ^{23}Na EFG values, suggesting that the tilt suppression is the primary structural role of barium cations. The fact that $^{47,49}\text{Ti}$ NMR spectra of BNT-xBT displayed negligible changes as a function of composition supports this hypothesis. Based on the present study, one may state that Ba^{2+} governs the tilting of rigid TiO_6 octahedra in this solid-solution, but does not influence the local structure of the Ti^{4+} cation by deformation of octahedra or changes in polar displacements of titanium.

CONCLUSION

$^{47,49}\text{Ti}$ NMR spectra of BNT-xBT samples with different barium content were investigated. Two important conclusions could be drawn based on the interpretation of these NMR spectra of titanium:

First, despite the fact that average structures are well-defined, the shape of the $^{47,49}\text{Ti}$ NMR spectra implies the local structure around the titanium site is strongly disordered, which may be a consequence of the random occupation of the A-site.

Second, the local structure around titanium nuclei remains invariant to the chemical modification with barium, in accordance with the effect reported for BNT modified with potassium.³¹ The lack of changes in the $^{47,49}\text{Ti}$ NMR spectra suggests the B-site of these perovskites is insensitive to the fine-tuning of the structure through the MPB caused by the addition of barium. This result implies that the chemical modification of BNT with Ba^{2+} does not lead to a significant distortion of the oxygen octahedra; instead, it impacts the local environment of the remainder A-site cations by suppressing the tilting of TiO_6 octahedra. These results confirm the expectations from a recent ^{23}Na NMR study of the local structure of BNT-xBT.¹⁰

SUPPLEMENTARY MATERIAL

See [supplementary material](#) for the details of the ECHODEPTH sequence and the effect of MAS on the line shape of the ^{47}Ti -NMR spectra.

ACKNOWLEDGMENTS

This work has been financially supported by the Collaborative Research Center SFB 595 “Electrical Fatigue in Functional Materials” of the Deutsche Forschungsgemeinschaft (DFG).

¹A. J. Moulson and J. M. Herbert, *Electroceramics: Materials, Properties, Applications*, 2nd ed. (John Wiley & Sons, Ltd, 2003).

²J. Rödel, W. Jo, K. T. P. Seifert, E.-M. Anton, T. Granzow, and D. Damjanovic, *J. Am. Ceram. Soc.* **92**, 1153 (2009).

³T. Takenaka, K. Maruyama, and K. Sakata, *Jpn. J. Appl. Phys., Part 1* **30**, 2236 (1991).

⁴H. D. Megaw, *Nature* **155**, 484 (1945).

⁵A. W. Hewat, *Ferroelectrics* **6**, 215 (1973).

⁶G. Shirane, H. Danner, and R. Pepinsky, *Phys. Rev.* **105**, 856 (1957).

⁷T. J. Bastow and H. J. Whitfield, *Solid State Commun.* **117**, 483 (2001).

⁸R. Blinc, V. Laguta, and B. Zalar, *Phys. Rev. Lett.* **91**, 247601 (2003).

⁹P. B. Groszewicz, H. Breitzke, R. Dittmer, E. Sapper, W. Jo, G. Buntkowsky, and J. Rödel, *Phys. Rev. B* **90**, 220104 (2014).

¹⁰P. B. Groszewicz, M. Gröting, H. Breitzke, W. Jo, K. Albe, G. Buntkowsky, and J. Rödel, *Sci. Rep.* **6**, 31739 (2016).

¹¹D. Padro, V. Jennings, M. E. Smith, R. Hoppe, P. A. Thomas, and R. Dupree, *J. Phys. Chem. B* **106**, 13176 (2002).

¹²N. Hao, B. G. Sayer, G. Dénès, D. G. Bickley, C. Detellier, and M. J. McGlinchey, *J. Magn. Reson.* **50**, 50 (1982).

¹³K. M. Chi, S. R. Frerichs, S. B. Philson, and J. E. Ellis, *J. Am. Chem. Soc.* **110**, 303 (1988).

¹⁴D. Padro, A. P. Howes, M. E. Smith, and R. Dupree, *Solid State Nucl. Magn. Reson.* **15**, 231 (2000).

¹⁵V. M. Goldschmidt, *Naturwissenschaften* **14**, 477 (1926).

¹⁶A. Glazer, *Acta Crystallogr., Sect. A* **31**, 756 (1975).

¹⁷I. M. Reaney, *J. Electroceram.* **19**, 3 (2007).

¹⁸G. O. Jones and P. A. Thomas, *Acta Crystallogr., Sect. B* **58**, 168 (2002).

¹⁹S.-T. Zhang, A. B. Kounga, E. Aulbach, H. Ehrenberg, and J. Rödel, *Appl. Phys. Lett.* **91**, 112906 (2007).

²⁰W. Jo, J. E. Daniels, J. L. Jones, X. Tan, P. A. Thomas, D. Damjanovic, and J. Rödel, *J. Appl. Phys.* **109**, 014110 (2011).

²¹C. Ma, X. Tan, E. Dul'kin, and M. Roth, *J. Appl. Phys.* **108**, 104105 (2010).

- ²²D. Massiot, F. Fayon, M. Capron, I. King, S. Le Calvé, B. Alonso, J.-O. Durand, B. Bujoli, Z. Gan, and G. Hoatson, *Magn. Reson. Chem.* **40**, 70 (2002).
- ²³D. G. Cory and W. M. Ritchey, *J. Magn. Reson.* (1969) **80**, 128 (1988).
- ²⁴T. Emmler, S. Gieschler, H. H. Limbach, and G. Buntkowsky, *J. Mol. Struct.* **700**, 29 (2004).
- ²⁵S. F. Dec, M. F. Davis, G. E. Maciel, C. E. Bronnimann, J. J. Fitzgerald, and S. S. Han, *Inorg. Chem.* **32**, 955 (1993).
- ²⁶A. Labouriau and W. L. Earl, *Chem. Phys. Lett.* **270**, 278 (1997).
- ²⁷T. J. Bastow, *J. Phys.: Condens. Matter* **1**, 4985 (1989).
- ²⁸C. Gervais, D. Veautier, M. E. Smith, F. Babonneau, P. Belleville, and C. Sanchez, *Solid State Nucl. Magn. Reson.* **26**, 147 (2004).
- ²⁹D. Freude, *Adv. Colloid Interface Sci.* **23**, 21 (1985).
- ³⁰R. Ranjan and A. Dviwedi, *Solid State Commun.* **135**, 394 (2005).
- ³¹V. A. Shuvaeva, D. Zekria, A. M. Glazer, Q. Jiang, S. M. Weber, P. Bhattacharya, and P. A. Thomas, *Phys. Rev. B* **71**, 174114 (2005).
- ³²B. N. Rao, L. Olivi, V. Sathe, and R. Ranjan, *Phys. Rev. B* **93**, 024106 (2016).

This article may be downloaded for personal use only. Any other use requires prior permission of the author and AIP Publishing. This article appeared in *Journal of Applied Physics* 121 (2017) 11 and may be found at <https://doi.org/10.1063/1.4978017>.

Available under only the rights of use according to UrhG.